Research

Numerical simulation for stress analysis of functionally graded adhesively bonded composite patch repair system

A. P. Khode[1] · S. V. Nimje[2]

© The Author(s) 2023   OPEN

Abstract

Three-dimensional finite element analyses have been carried out for adhesively bonded composite patch repaired an aluminum alloy plate structure with centre circular notch. Presence of defect in the plate causes stress gradients in the bond region which results in reduction of the performance of the patched panel. The patterns of out-of-plane stress components at various interfaces (plate-adhesive-patch) at different angular positions with reference to loading direction are evaluated for mono-modulus adhesive. In the present research work, an attempt has been made to improve the strength of adhesively bonded composite patch repaired system by reducing stress concentration at the critical regions. This has been achieved by smoothening/relieving stresses over the entire bond region by introducing functionally graded adhesive (FGA) material in-lieu of conventional mono-modulus adhesive. Linear material gradation function profile has been used to tailor adhesive layer in the bond region. Effect of material gradation profile with different modulus ratios on out-of-plane stresses at different interfaces of composite patch repaired system have been studied. Numerical simulations based on FE analyses indicates significant reduction in out-of-plane stress levels by which strength of functionally graded composite patch repaired system will be enhanced.

Keywords Composite patch repair · Functionally graded adhesive · Elastic modulus ratio · Out-of-plane normal · Shear stress

1 Introduction

Aircraft structures are much optimised structures. But when these are subjected to severe loading due to wind gust, ground reactions during take-off and landing, manoeuvres, accelerations, bird strike etc., may cause damage to the structures. In order to increase the life of the structure, one has to do restoration. Main objective behind the repair is that to make the component functional and it should not cause the catastrophic failure of the whole assembly. There are many methods of restoration of the damaged aircraft structure. One of the economical ways of restoration is mechanical repairs. Modern trend in repairs of aircraft structure recommend use of adhesively bonded joints. Bonded repairs have advantages like reduced stress concentrations, improved fatigue life, light-in-weight. This is very versatile method which can be used for joining of large range of materials and dissimilar materials also. It can be used for variety of interfaces like metal-to-metal, metal-to-composites and composite-to-composite.

✉ S. V. Nimje, sunil.nimje@diat.ac.in | [1]Vehicles Research & Development Establishment (VRDE), DRDO, Ministry of Defence, PO Vahannagar, Ahmednagar 414006, India. [2]Department of Mechanical Engineering, Defence Institute of Advanced Technology (DIAT), Girinagar, Pune 411025, India.

In adhesively bonded patch repair, adhesive layer is used to connect patch and parent structure which ensures stress and deformation transfer between them. Hence, adhesive film experiences different types of stresses like shear, tension, cleavage & peel. The adhesive film is experienced by high stress gradients at the overlap ends due to change in stiffness [1]. The peel and shear stress distribution in the adhesive layer are not uniform. These stresses have maximum value at the overlap end which cause stress concentration. This results in reduced fatigue life and de-bonding which ultimately reduces the overall patch repair efficiency and performance. Hence, to improve the performance of patch repair system, the stress gradients need to be reduced. Stress concentration can be reduced by redistribution of the stresses over the bond area.

Gu et al. [2] determined the behaviour of bonded composite patch repair for aluminium substrate through numerical method. Boron/epoxy patches absorb dissipated energy. Reduction in adhesive thickness reduces the SIF in the panel due to more transfer of load from panel to patch. Marioli-Riga et al. [3] explained analysis methodology for the design of composite patch repairs required for damaged metallic components. This methodology has resulted into a single design algorithm. It shows systematic way to guide the designer through the design/analysis process. Mohammadi et al. [4] concluded two-sided patch efficiency is higher than the one-sided patch. Similarly, the composite patch efficiency is higher than the metal patch. Tsamasphyros et al. [5] carried out study on composite patch repair by analytical and numerical methods. Rose model is simple but it is limited to simple geometries still it can be useful to do design approximations in early stages of design and calculate remaining life of the component. Rodríguez et al. [6] observed load achieved in patched specimens is twice than unpatched. Sand blasting of bonding surface improves the adhesion between steel and composite. Yang et al. [7] observed that angle of the repair plays an important role in composite patch repairs of the scarf joint. Lee et al. [8] studied the effects of different patch shapes in composite patch repairs. For inverted triangular patch shape, bonding strength is improved. Wang et al. [9] studied analytical method for stepped scarf patch repair. The model accurately predicts stress distribution along the bondline.

Cohesive zone modeling has been widely used in recent years to predict fracture in adhesive joints and composite laminates [10]. Cohesive process zone models can deal with the nonlinear zone ahead of the crack tip due to plasticity or micro-cracking present in many materials. Precise determination of the traction–separation laws is very crucial to the completion of the cohesive zone model. Cohesive behavior specified directly in terms of a traction–separation law can be used to represent the delamination at interfaces in composite laminates and enables the specification of material data such as the fracture energy as a function of the ratio of normal to shear deformation (mixed mode) at the interface. Within the cohesive model, the damage and fracture of a structure are modeled by a damage-free bulk material and special interface elements (cohesive elements). Ghabezi and Farahani [11] assessed the effects of nanoparticles on bridging laws, cohesive mechanism and traction–separation parameters of nanocomposites mode-I and II fracture. To do this analyzing of the experimental data from double cantilever beam, and end notched flexure tests including construction of the R-curves (energy release rate versus crack length), reconstruction of these curves in terms of the pre-crack tip opening and sliding displacement, and calculation of the corresponding bridging and traction–separation laws through the J-integral approach were carried out.

Vadean et al. [12] examines the effects of the different parameters on the stress state in the patch adhesive, such as ply orientation, stacking sequence, ply thickness and scarf angle. Theyexplored an adaptive design of the repair patch for orthotropic materials and composite laminates, using 3D finite element analysis. The optimization method and the improved shapes were presented and discussed with respect to the influencing parameters. Shinde et al. [13] repaired thin panels of aluminium alloy 6061-T6 with a centre pre-crackwith a one-sided asymmetrical CFRP patch through co-curing of epoxy at the room temperature to have minimal residual stresses. The specimens were tested with a tension-tension fatigue load. The numerical simulation as well as the experiments showed that the fatigue life was improved considerably with the increasing patch length when tested at room temperature. Borges et al. [14] discussed the progresses in adhesive materials, divided into structural and non-structural adhesives, and highlighted advances insecond-and third-generation acrylics, toughened epoxies, and two-component polyurethanes for structural applications, and pressure-sensitive adhesives and bio-adhesives in the non-structural category. Afterwards, novel joint designsand manufacturing concepts are discussed, including functionally graded joints, hybrid joints, self-dismantling joints, and additive manufacturing applied to adhesive joints. Uslu and Kaman [15] repaired carbon fiber-reinforced U-notched composite plates with composite patches made of the same material using adhesive bonding and their mechanical performance was investigated experimentally and numerically. Repairs were made by applying a double-sided composite patch to the notched thin composite plates. The repaired composite plates were tested under tensile load. The effect of the variation in notch width and depth on the repaired plate failure load and type was investigated. Ghabezi and Farahani [16] performed experimental investigation and comparison between different bridging laws. For mode-II

fracture in the presence of nano-particles, these laws are calculated from three data reduction schemes for describing the bridging zone and trapezoidal traction–separation law parameters. For the calculation of the energy release rate in mode-II fracture, three corresponding data reduction schemes, compliance calibration method, corrected beam theory and compliance-based beam method, have been utilized for different percentages of nano-particles in the adhesives and the adherends. Moreira et al. [17] addressed the behaviour of aluminium adherends repaired with CFRP patches under quasi-static and fatigue loading analysis. Three types of bonded repairs, single-strap, double-strap and scarf were evaluated under three-point bending loading. Representative load–displacement curves in the quasi-static case and compliance versus number of cycles curves under fatigue loading were obtained. The purpose was to determine the static strength and fatigue lives for the three repair geometries. Numerical analyses considering two different cohesive zone models, suitable for quasi-static and fatigue loading, were carried out. The aim is to compare the numerical predictions with the experimental results for all analysed cases, targeting to validate appropriate numerical procedures to deal with quasi-static and fatigue behaviour of bi-material bonded repairs. Truong et al. [18] investigated the failure of scarf patch-repaired composite laminates with different scarf angles and subjected to different bending loads. An experimental program was proposed as well as a finite element model simulation with cohesive zone modeling. The failure loads, including the crack initiation and propagation process, which was extremely difficult to observe in experiments, were considered in detail with the finite element model simulation.

Carbas et al. [19] have carried out study on repair of wood structures. They used functionally graded bond line by using methodology of graded cure of adhesive. This imparts gradation of elastic modulus along the bond line. At high stress concentration area, adhesive with low elastic modulus is used while stiff adhesive is used in the area where high strength is required. They carried out numerical simulation and results validated with experimental set-up. Their results depicted that gradation of adhesive elastic modulus can improve strength and reliability of the component. Marques et al. [20] carried out simulation of double lap joint of aluminium alloy specimen. They provided internal taper at the edges and also used dual adhesives for gradation of adhesive. The strength is improved for the components, which have been provided with taper as compared to that of taper-less configuration. Combination of ductile adhesive (2015) and brittle adhesive (AV138) imparts synergetic effects. Joints with dual-adhesive have strength as equivalent to that of stiff adhesive alone. This can be useful during dynamic loading, where there is requirement of ductile adhesive which can withstand the shocks at the same time stiff adhesive can provide the strength. Breto et al. [21] varied adhesive properties along the bond line. Study was carried out for improvement of strength for aluminium and composite joint under shear loading. Material tailoring of bond line is helpful even for discrete models also. They could able to show improvement in the joint strength in order of 70% as compared to that of mono-modulus adhesive. Paroissiena et al. [22] observed gradation of elastic modulus can reduce the peak adhesive stresses. They propose gradation of properties for adhesive as well as for adherend in order to improve the strength of single lap joints. Khan et al. [23] carried out numerical simulation of a through-thickness defect repaired with circular patch. They compared results of the considered repaired structure with mono-modulus bondline (MMB) to that of functionally modulus graded bondline (FMGB). By using FMGB stress concentration at defect and edges of the patch are redistributed to ensure uniform distribution of stress and reduce peak adhesive stresses along the bond line. Srinivasan et al. [24] carried out finite element analysis and experimental tests for single lap joint using bi-adhesive. They used AF3109 and EA9696 for tailoring of the joint. The failure strength of the joint is improved by 51.64%. Failure mode changes from adherend fibre tear to cohesive failure of adhesive due to tailoring of the bond line. Nimje and Panigrahi [25] carried out three-dimensional non-linear finite element analyses of adhesively bonded double supported tee joint. Strain energy release rates (SERR) were used to determine damage growth parameters. Damage initiation takes place at interface of the adhesive layer and base plate. Use of functionally graded adhesives showed significant lowering of the damage growth parameters. Increase in modulus ratio causes more decrease in these damage growth driving forces.

Dugbenoo et al. [26] proposed to use additive manufacturing (AM) technique for material tailoring of the joint. AM tailoring increases surface area available for bonding. The AM tailored joint showed 5.5 times improvement in strength as compared to baseline single lap joint. Nakanouchi et al. [27] used mixing of two types of acrylic adhesives for tailoring of the bondline. Ratios of two adhesives were varied to check the adhesive properties. They used applicator for adhesives for physical testing. Increase in ratio of hard adhesive increases modulus of elasticity while on other hand decreases the failure strain of the adhesive. Hence it is possible to manufacture adhesive layer with gradation of the properties. Marques et al. [28] discussed latest technologies in design and manufacturing of FGA. They suggested gradation of adhesive by embedding particles in the adhesive, differential curing of the bondline and adhesive mixing. Gradation enhances mechanical properties such as strength, stiffness, toughness along the bondline. The ability to tailor the adhesive open a facet in engineering design by using sophisticated and high-performance adhesive bond. Silva et al. [29] manufactured

adhesive layer containing iron micro-particles and used magnetic field to create a graded particle distribution along the overlap region. Iron micro-particles can effectively be used to enhance the mechanical properties of adhesive in a joint, although the effectiveness of this reinforcement is highly dependent on the particle amount and distribution. They also validated numerical simulation against experimental data. Rudawska [30] studied effects of curing methods on mechanical properties of the joint. She observed high temperature curing is advantageous for the strength of the joint.

From the above literature survey, it is clear that in composite patch repairs using mono-modulus adhesive causes stress concentration. Very few literatures are available for reducing stress concentration for the patch-repaired system. In the present work, numerical simulation of stress analyses are performed for Aluminium alloy (2024-T3) plate with circular notch repaired by functionally graded adhesively bonded composite patch using finite element analysis. FE model of the patch repaired system has been validated with published results available in literature. Systematic parametric study has been performed with various modulus ratios in order to investigate their effect on out-of-plane stresses at different interfaces of composite patch repaired system.

2 Finite element modeling and analysis of composite patch repair system

2.1 Geometric modelling

Geometry of the repair configuration of the plate is shown in Fig. 1. It consists of rectangular plate of length (L) 160 mm, width (W) 40 mm and thickness (t_1) 2 mm. Material of the plate is aluminium alloy 2024-T3. This plate consists of through thickness circular notch of diameter (d) 5 mm. The plate is subjected to uniform tensile load (F_1) of 8 kN. The origin of coordinate system is located at centre of hole and middle of plate across thickness. The material properties of plate are given in Table 1. The plate is repaired with composite circular patch. The diameter (D) of the patch is 25 mm and thickness (t_3) is 2 mm. The patch consists of 4 layers of boron/epoxy composite lamina each having thickness of 0.5 mm with fibre orientation of [45/-45/45/-45]. Layer wise orthotropic material properties of boron/epoxy lamina in principal material direction are given in Table 2.

The patch is bonded with the plate from both sides similar to symmetric repair. The adhesive film of thickness (t_2) 0.1 mm is used for bonding of patch with the plate. In present work, two types of adhesives namely mono-modulus and functionally graded adhesives are used to bond the patch with defective plate structure. The properties of mono-modulus adhesive are given in Table 3. The details of functionally graded adhesive considered in the present work are extensively discussed in proceeding section.
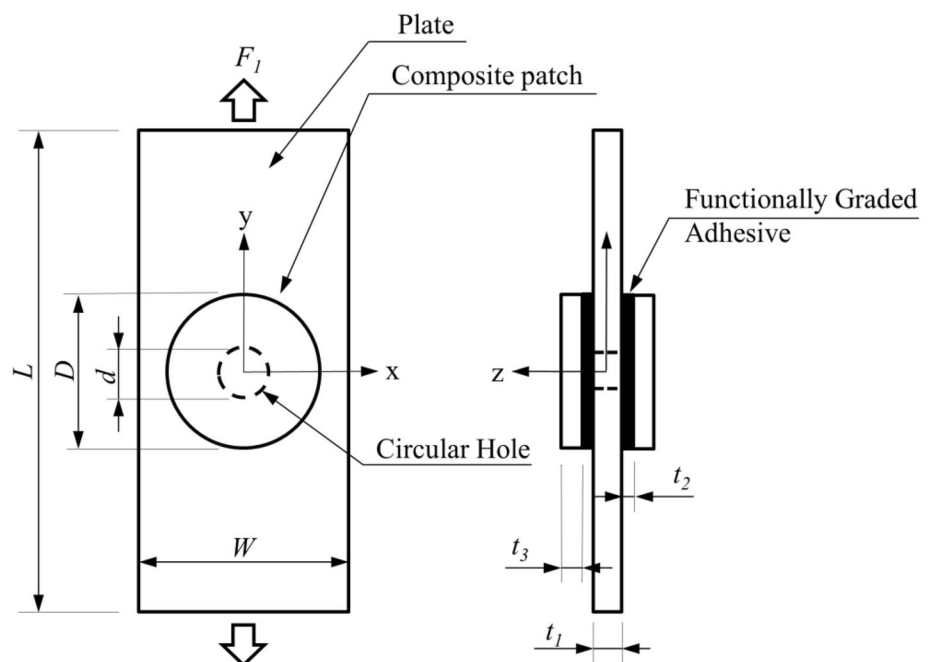
Fig. 1 Geometry of the patched plate structure

Table 1 Material properties of aluminium alloy 2024-T3 [31]	Property	Value
	Modulus of elasticity (E)	71.02 GPa
	Poisson's ratio (v)	0.3
	Elongation at break	15%
	Density (ρ)	2700 kg/m^3
	Yield strength (σ_y)	320 MPa
	Ultimate strength (σ_u)	480 MPa
	Fracture toughness (K_{IC})	25 MPa $\sqrt{m}$

Table 2 Layer-wise orthotropic material properties of boron/epoxy composite lamina in principal material direction [32]	Property	Value
	Modulus of elasticity	
	E_x	208.1 GPa
	$E_y = E_z$	25.44 GPa
	Poisson's ratio	
	$v_{xy} = v_{xz}$	0.1677
	v_{yz}	0.36
	Shear modulus	
	$G_{xy} = G_{xz}$	7.2 GPa
	G_{yz}	4.9 GPa

Table 3 Elastic properties of epoxy adhesive [25]	Property	Value
	Modulus of elasticity (E)	2.8 GPa
	Poisson's ratio (v)	0.4

2.2 Modeling of bond region with functionally graded adhesive (FGA)

Many researchers [33–35] considered linear and exponential function profiles for functionally graded materials. The same authors have used FGA materials in the earlier work [33]. One of the objectives was the optimization of the suitability of graded profile (linear or exponential) by comparing the magnitude of the stress components for out-of-plane joint structure. It was clearly spelt out that the linear material gradation function profiles offer a better reduction in magnitude of peak values of peel stress based on 3D FE analysis. Again, the same authors have analysed the effects of exponential and linear material gradation profiles on stress intensity factors (SIF) in their earlier work [36]. It was observed that the SIF reductions are more pronounced for linear material gradation profile compared to that of exponential profile. Also, Chandran and Barsoum [34] suggested the advantages of usingfunctionally graded material with liner function profile based on the SIF value for a finite-width functionally graded plate with embedded crack.

The aforesaid reasons justified the use of linear function profile in the present research for improved structural performance of patch repaired system. Since, the structural performance in case of functionally graded adhesively bonded patch repaired system largely depends on the peak vales of stress levels and SERR. Significant reductions in those values are observed due to use of linear graded function profile. Hence, in the present investigation, continuous variation of elastic modulus of adhesive along the bond region has been considered. The smooth variations of bond region modulus have been implemented by applying a number of rings of adhesive of different moduli in the bond region which is expressed by following linear function profile [34]:

$$E(r) = E_1 - \frac{2 \times (E_1 - E_2)}{(r_o - r_i)} \times |r - r_m| \tag{1}$$

where,

$E(r)$-Modulus of elasticity at instantaneous bond radius (r).

r_o-Outer radius of the adhesive.

r_i-Inner radius of adhesive.

r_m-Mean radius of adhesive which is given by

$$r_m = \frac{(r_o + r_i)}{2} \qquad (2)$$

Material gradients are evaluated in terms of modulus ratio (R) which is expressed as follows:

$$R = \frac{E_1}{E_2} \qquad (3)$$

where,

E_1-Modulus of elasticity for stiff adhesive.

E_2-Modulus of elasticity for flexible adhesive.

It was assumed that the relationship between the Young's modulus and shear modulus remains constantinvariably with grading or, in other words, Poisson's ratio 'v' remains constant [34]. Figure 2 shows the representative functionally adhesive layers in the bond region with different terminologies used in the above equation. The elastic modulus ratios used in present work are 1, 1.5, 2, 4 and 6. The elastic modulus ratio 1 corresponds to the mono modulus adhesive where the elastic modulus is constant. The elastic modulus ratios 1.5, 2, 4 and 6 are graded adhesive where the modulus of adhesive varies linearly for different radii of adhesives as shown in Fig. 3

2.3 Meshing scheme

2.3.1 Plate

The plate is modelled with solid elements. Two dimensional elements are generated on the front face of the plate. Around hole, 120 elements are created. In the patch region, size of the element in radial direction is kept constant. These 2D elements are then dragged along the thickness direction to generate volume. In the thickness direction, six elements are generated. The eight noded brick elements called structural SOLID 185 from ANSYS, are used for discretization of the geometry. Figure 4 illustrates views of meshing scheme of repaired plate structure.
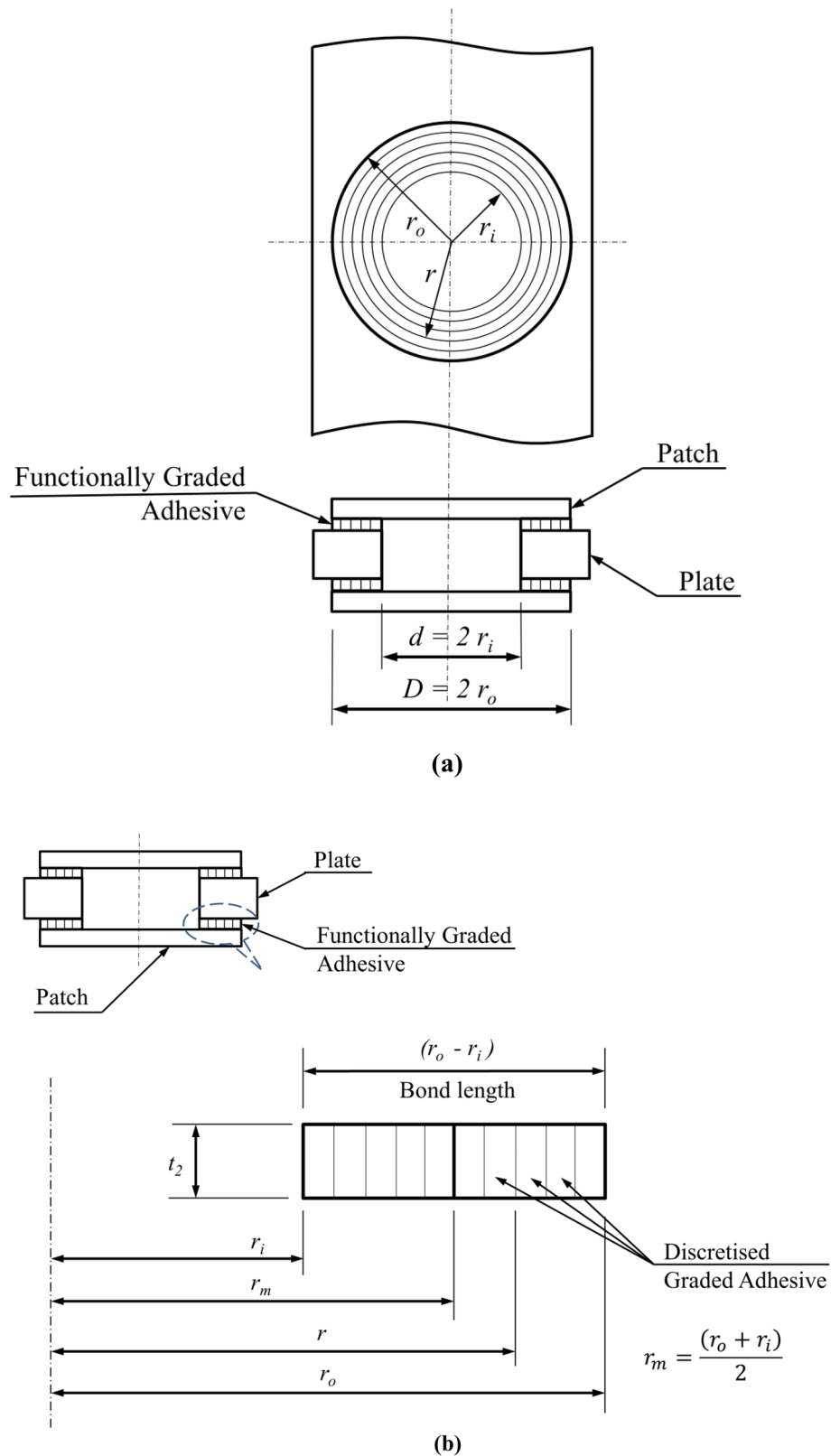
2.3.2 Composite patch

The composite patch is modelled with three-dimensional solid elements (SOLID 185). The pattern of area meshing of patch/adhesive interface is generated similar, so that it can be easily coupled with respect to each other at the interface. The patch is made of composite laminate having different lay-up orientation, the layer angles are defined by assigning the element coordinate system to the patch elements. Each layer is assigned one element in thickness direction. It is assumed that patch/adhesive interface is perfectly bonded; hence the nodes are coupled at the interfaces to reflect the perfectly bonded behaviour. Figure 5 illustrates FE model of composite patch.

2.3.3 Functionally graded adhesive

Similar to composite patch, functionally graded adhesive is modelled with three-dimensional solid elements (SOLID 185). The pattern of area meshing of adhesive/patch and adhesive/plate interfaces is generated similar, so that it can be easily coupled with respect to each other at the interface. It is assumed that adhesive/patch and adhesive/plate interface is perfectly bonded hence the nodes are coupled at the interfaces to reflect the perfectly bonded behaviour. The meshing scheme of adhesive is highlighted in Fig. 6.

For modelling of patch repaired system with functionally graded adhesive, the region of adhesive is assumed to have a Young's modulus changing along the radial direction using Eq. (1).In finite element model, the changes of material property have been modelled discretely, by assigning the value of $E(r)$ at the middle for each of the elements [34] within the adhesive layer. The smooth variation of elastic moduli is ensured by keeping fine mesh (mesh size tends to zero)

Fig. 2 Adhesive modelling-terminologies; **a** Adhesive model with plate and patch interface, **b** Bond region

Functionally Graded Adhesive

Patch

Plate

$d = 2\,r_i$

$D = 2\,r_o$

(a)

Plate

Functionally Graded Adhesive

Patch

$(r_o - r_i)$

Bond length

t_2

r_i

r_m

r

r_o

Discretised Graded Adhesive

$r_m = \dfrac{(r_o + r_i)}{2}$

(b)

along the bond region. One hundred material properties are created for gradation of adhesive elastic modulus. For this purpose, a MATLAB code is generated. Output of this code is used in Mechanical ANSYS Parametric Design Language (Mechanical APDL) for creating material model and assigning it to respective elements based on spatial coordinates.

Fig. 3 Variation of elastic modulus along bond region for different modulus ratios 'R'
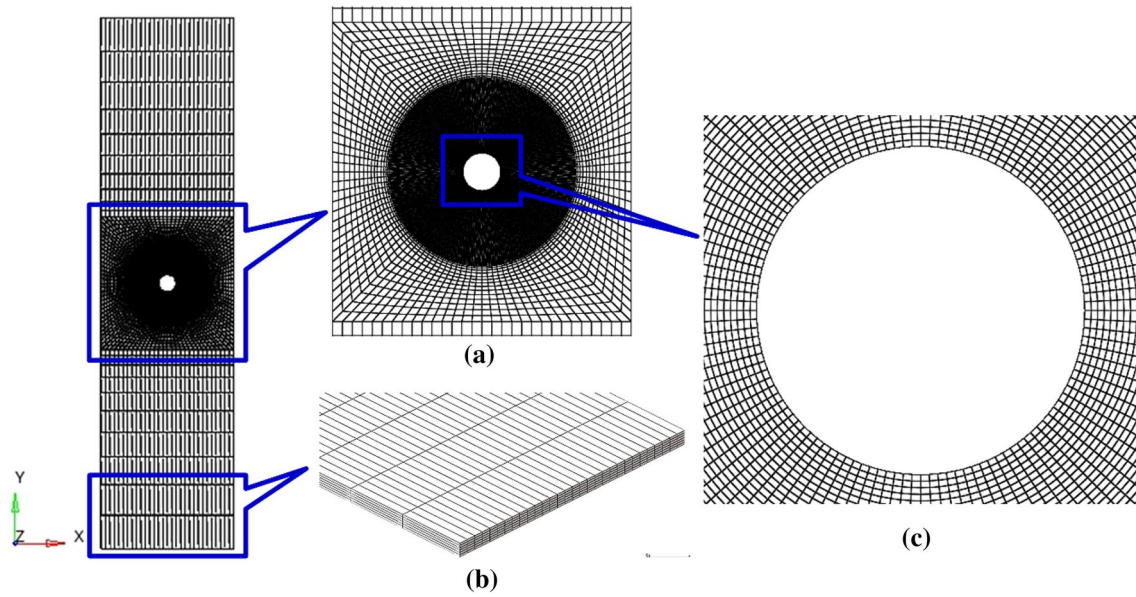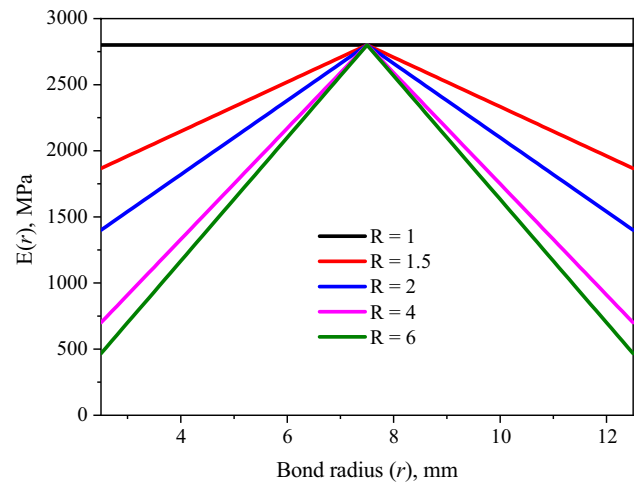
Fig. 4 FE model of plate structure; **a** enlarged view around centre, **b** enlarged view around bottom edge, and **c** enlarged view around hole different modulus ratios '*R*'
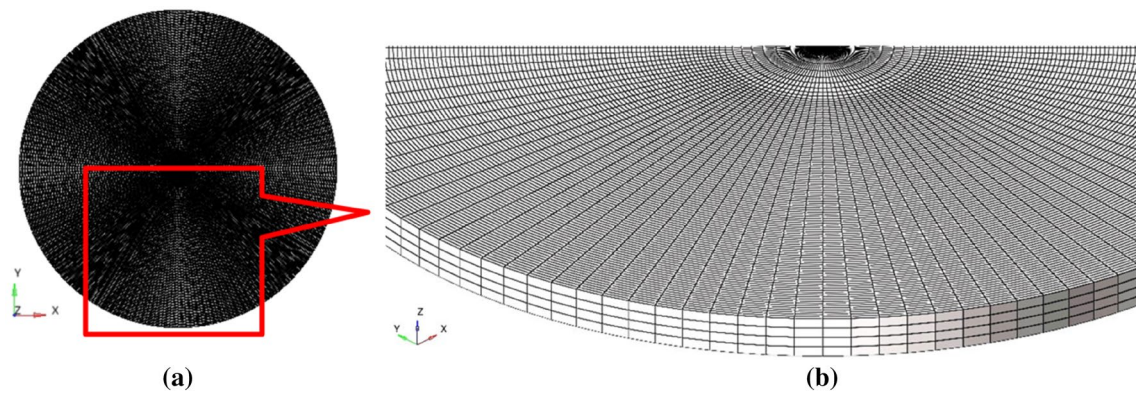

Fig. 5 FE Model of composite patch; **a** full model, and **b** zoomed view
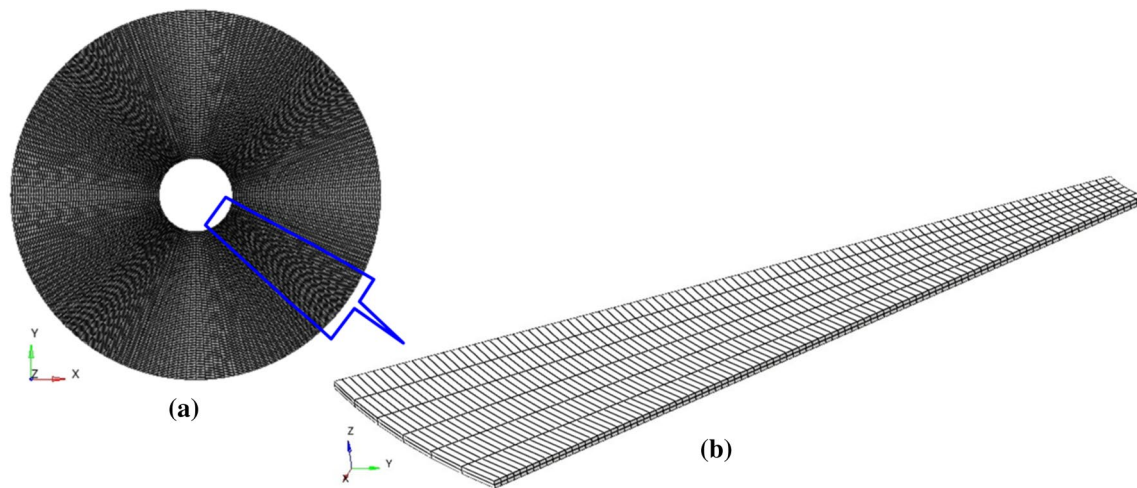
Fig. 6 FE model of adhesive; **a** full model, and **b** enlarged view

2.3.4 Boundary conditions

Boundary conditions applied to the configurations of the FE model shown in Fig. 7 are summarised in Table 4.

2.3.5 Validation of FE model

In the present work, FE model is validated by comparing the results with available literature by considering aluminium plate with circular defect repaired by circular patch made of graphite/epoxy.The out-of-plane shear stresses in the adhesive layer are evaluated and compared with those obtained from Madani et al. [37]. Referring to Fig. 8, the distribution of out-of-plane shear stress at mid-surface of adhesive layer of patch repair system shows good agreement with the available results.

3 Results and discussions

3.1 Stress analysis of patch repaired structure with mono-modulus adhesive

The stresses in adhesive film for mono-modulus adhesive ($R = 1$) are not uniform. Adhesive stress is more at the edges of hole and patch. The stress values vary from 37.2 MPa at edges to 2.9 MPa away from the edges. This much large variation is observed in the adhesive layer. This causes stress concentration in adhesive layer. Similar behaviour was observed by Khan et al. [23]. Similarly, the stress values are not uniform with reference to loading directions. Adhesive stresses are varying with reference to loading axis. Also, across the thickness of the adhesive, stress values are varying.

Variations of out-of-plane normal stress (σ_z) and shear stress (τ_{yz} & τ_{xz}) components are obtained for mono-modulus adhesive ($R = 1$). The stress components are plotted as a three-dimensional graph at different bond radius and angular position with loading axis. These plots are obtained for three different positions along thickness of adhesives that is adhesive-plate interface, mid adhesive layer and adhesive- patch interface. The stress pattern for out-of-plane normal stress (σ_z) and shear stress (τ_{yz} & τ_{xz}) components, among all these three interfaces are similar but values are different. Out of these three interfaces, Fig. 9 shows stresses for mid adhesive layer.

Referring to Fig. 9a, out-of-plane adhesive stress (σ_z) varies from maximum negative value at bond radius ($r = 2.5$) to maximum positive value at bond radius ($r = 12.5$). These locations are edge of hole in the panel and edge of the patch respectively, which causes stress concentration in the adhesive layer. The normal stress (σ_z) in adhesive away from the stress concentration zone is nearly constant for remaining bond region. At extreme bond radius that is at edge of the hole and edge of the patch, normal stress (σ_z) can be observed. Here, variation of adhesive normal stress (σ_z) at different angular positions can be seenclearly. Along different angular positions with reference to the loading axis, adhesive normal stress (σ_z) value is varying smoothly. Along the loading direction that is at the angle of 0° and 180° stress value is
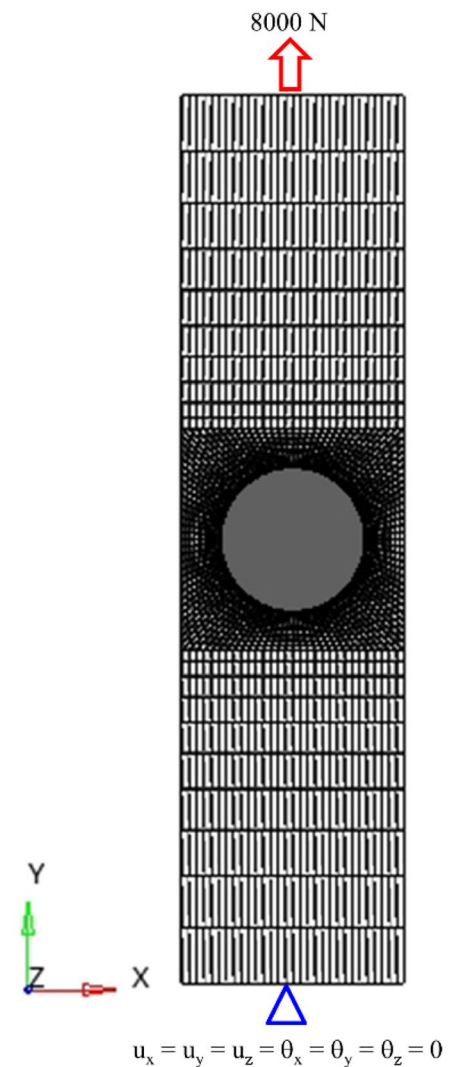
Fig. 7 Boundary conditions
for the model

$$u_x = u_y = u_z = \theta_x = \theta_y = \theta_z = 0$$

Table 4 Boundary conditions applied to FE model

Location	Boundary condition
Lower surface of plate	$u_x = u_y = u_z = 0$ $\theta_x = \theta_y = \theta_z = 0$
Upper surface of plate	Force in +y direction 8000 N

higher, while it is lower for the direction perpendicular to the loading axis that is at the angle of 90° and 270°. Away from the edges of the hole and patch, effect of angular position with loading axis on adhesive normal stress (σ_z) is negligible.

Out-of-plane shear stress (τ_{yz}) distribution is shown in Fig. 9b. The value of this stress component is maximum negative value at angular position of 0° with the loading axis to maximum positive value at angular position of 180° with the loading axis. Similar behaviour of this stress component is observed for different bond radius but it is having higher values at bond radius ($r = 2.5$) and ($r = 12.5$) and lower values at bond radius ($r = 7.5$). Also, at angular position on 0° against different bond radius, the variation of this stress component is smooth curve similar to semicircle which is having maximum negative value at bond radius ($r = 2.5$) and ($r = 12.5$) and minimum value at mean bond radius ($r = 7.5$). Similar pattern of stress is observed at angular position of 180° but here stress values are positive.

The shear stress (τ_{xz}) component variation with bond radius and angular position with the loading direction is seen in Fig. 9c. As compared to other two stress components (σ_z &τ_{yz}) the magnitude of this shear stress (τ_{xz}) is smaller and the stress pattern is different. At extreme bond radius variations of this stress shows different behaviour with different
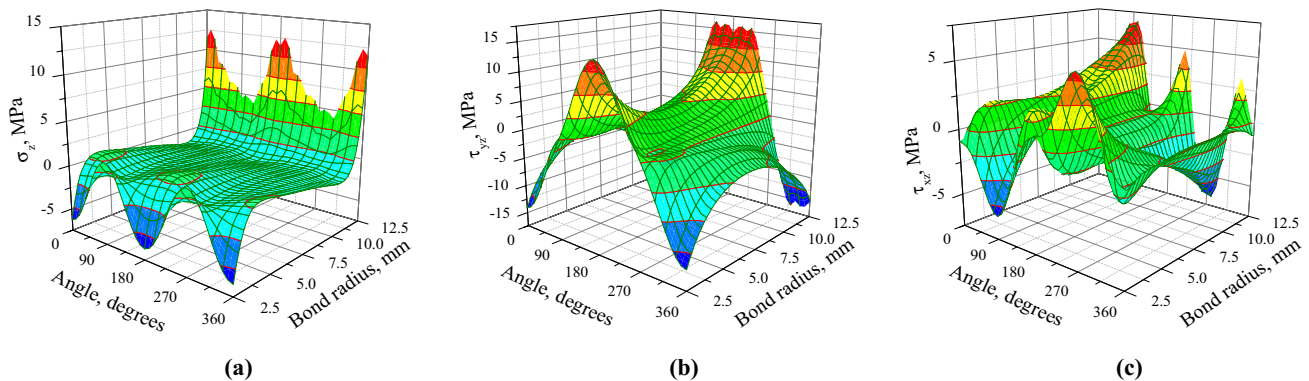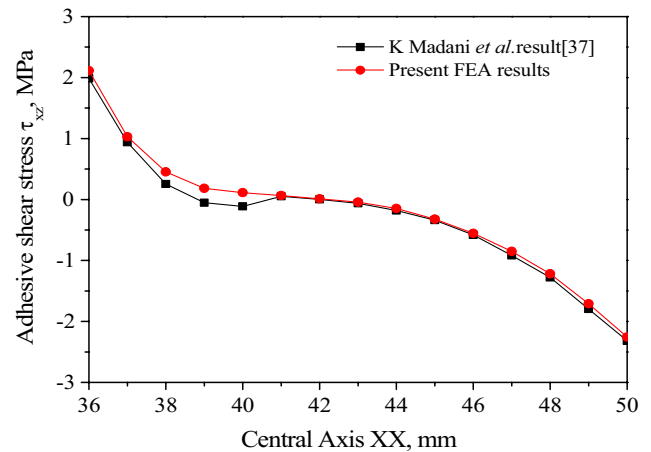
Fig. 8 Variation of the adhesive stresses (τ_{xz})

Fig. 9 Out-of-plane stress distribution at mid-adhesive layer along bond radius and different angular positions **a** Normal stress, σ_z, **b** Shear stress, τ_{yz} and **c** Shear stress, τ_{xz}

angular positions. For this stress, minimum value is observed in the loading direction that is at 0° & 180° while maximum value is observed at 90° & 270°.

In Fig. 9, we have seen the adhesive stresses at mid-adhesive layer. Interfacial stresses are also obtained at adhesive-patch interface and adhesive-plate interface. Figure 10 shows the out-of-plane normal stress (σ_z) at extreme bond radius ($r = 2.5$ & $r = 12.5$) and at different interfaces such as mid of adhesive layer, adhesive-patch and adhesive-plate interfaces. The pattern and nature of the adhesive normal stress is similar along thickness of the adhesive but values of the stresses are different. At the adhesive-plate interface, the value of adhesive normal stress (σ_z) is higher compared to other two positions along the thickness of the adhesive and it is having lower value at the adhesive-patch interface.

Out-of-plane shear stress (τ_{yz}) at the edge of the hole ($r = 2.5$) and the edge of the patch ($r = 12.5$) is shown in Fig. 11a, b respectively. At edge of the hole ($r = 2.5$) there is not much variation in this stress component across the thickness of the adhesive. While at the edge of the patch ($r = 12.5$), the value of adhesive shear stress (τ_{yz}) is slightly higher at adhesive-patch interface, as compared to other two positions along the thickness of the adhesive.

Similarly, the shear stress (τ_{xz}) variation in the adhesive layer at boundaries that is at edge of the hole ($r = 2.5$) and edge of the patch ($r = 12.5$) is shown in Fig. 12a, b respectively.

The behaviour of this stress component (τ_{xz}) is not similar across the extreme bond radius. But peak value in the stress observed at the extreme bond radius only. At the bond radius ($r = 2.5$), shear stress (τ_{xz}) varies from maximum in negative direction at angular position of 90° with the loading axis to maximum in positive direction at angular position of 270° with the loading axis. At bond radius ($r = 12.5$), the shear stress (τ_{xz}) varies with the direction of the load but having peak stress value at angular position of 90° and 270° similar for that of bond radius of ($r = 2.5$) but opposite in nature. Along bond radius for angular position of 90° the nature of this stress changes from maximum negative value at bond radius ($r = 2.5$) to maximum positive value at bond radius ($r = 12.5$). Similar behaviour is observed at angular position of 270° but the nature of the stress is opposite. Similar to shear stress (τ_{yz}) component, the value of adhesive shear stress (τ_{xz}) is slightly higher at adhesive-patch interface along the thickness of the adhesive.
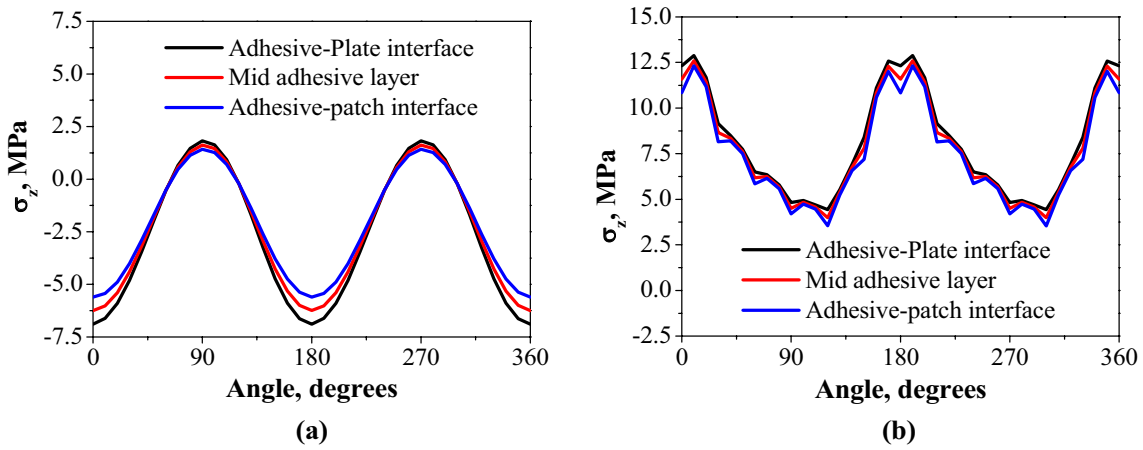
Fig. 10 Out-of-plane normal stress (σ_z) distribution for three interfaces at different angular positions along bond radius; **a** $r=2.5$, **b** $r=12.5$
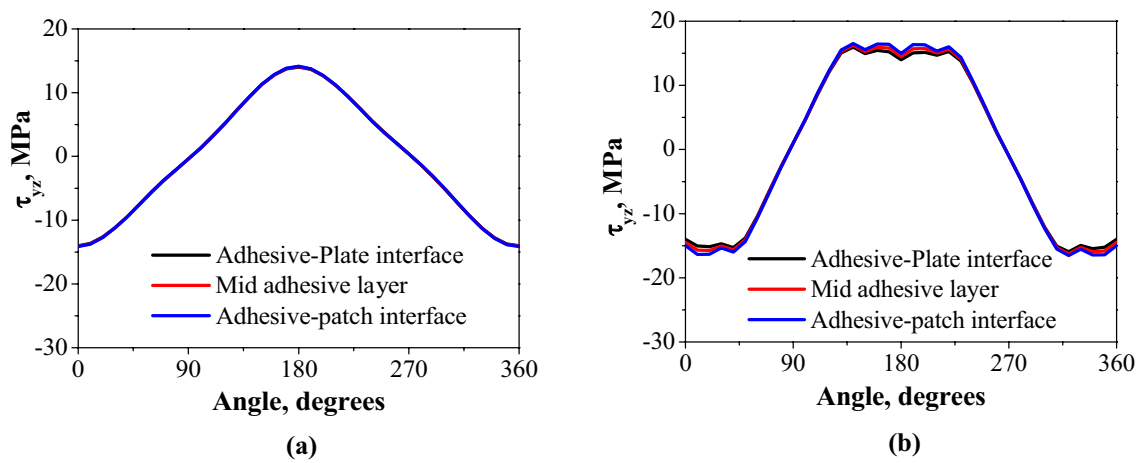

Fig. 11 Out-of-plane shear stress (τ_{yz}) distribution for three interfaces at different angular positions along bond radius; **a** $r=2.5$, **b** $r=12.5$
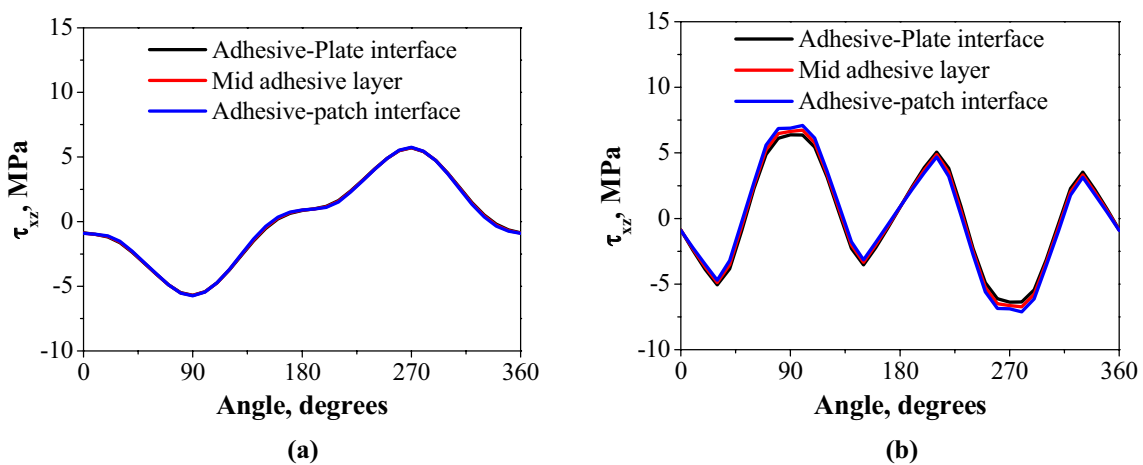

Fig. 12 Out-of-plane shear stress (τ_{xz}) distribution for three interfaces at different angular positions along bond radius; **a** $r=2.5$, **b** $r=12.5$

As observed in above discussion the stress components (σ_z & τ_{yz}) have maximum value in the direction of the load. Hence, this direction is considered for comparing stresses for different elastic modulus ratios (R).

Variation in adhesive stresses were observed along the thickness of the adhesive layer. The normal stress (σ_z) have maximum value at the adhesive-plate interface. The value is 18% higher at the edge of the hole as to that of other interfaces. The shear stress components (τ_{yz} & τ_{xz}) have maximum value at the adhesive-patch interface. The variation of about 4–6% observed for the shear stresses as compared to other interfaces. Adhesive stresses are having intermediate value at the adhesive mid layer.

3.2 Stress analysis of patch repaired structure with functionally graded adhesive

In earlier section we have discussed about stress distribution in conventional mono modulus adhesive ($R=1$) where adhesive properties are constant with reference space coordinates. The stresses within the adhesive layer are not uniform. Stresses are more at the boundaries of the adhesive which causes stress concentration. Due to availability of the modern manufacturing techniques for production of functionally graded adhesive, it is feasible to change the properties of the adhesive with reference to space coordinates. Hence effect of change in adhesive elastic modulus is discussed in this section.

Figure 13 shows out-of-plane normal stress (σ_z) distribution along bond radius for different elastic modulus ratios (R) of adhesive. The variation in normal stress component is maximum negative value to maximum positive value at bond radius ($r=2.5$) and ($r=12.5$) respectively. The normal stress value is nearly constant or near to zero between bond radius ($r=5$) and ($r=10$). For elastic modulus ratio ($R=1$) the peak stress obtained at the edges of hole and patch is higher. As the modulus ratio increases from ($R=1$) to ($R=6$) the peak adhesive stress observed at the edges of hole and patch reduces. The pattern of variation in normal stress across bond radius is similar for different elastic modulus ratios (R). The effect of reduction in peak adhesive normal stress at the stress concentration zone is promising. While away from stress concentration zone that is between bond radius ($r=5$–10) there is smaller change in the adhesive stress due to gradation of adhesive elastic modulus. For higher elastic modulus ratio (R) the adhesive normal stress across the bondregion between bond radius ($r=2.5$–12.5) becomes more uniform. Hence, at the edges where there is stress concentration zone, low elastic modulus adhesive can be used to reduce higher adhesive stress observed at the edges. Similarly at the interior, away from the edges where there is no much change due to gradation of adhesive elastic modulus, high elastic modulus can be used. This will help to carry more load.

Out-of-plane shear stress (τ_{yz} & τ_{xz}) distribution along bond radius for different elastic modulus ratios are shown in Figs. 14, 15 respectively. Shear stress (τ_{yz} & τ_{xz}) is maximum at the edges for mono modulus ($R=1$) adhesive and variation between maximum & minimum stress along bond region is also higher for this adhesive. Similar to normal stress, the pattern of variation in shear stress across bond radius is similar for different elastic modulus ratios (R). As the elastic modulus ratio increases the shear stress (τ_{yz} & τ_{xz}) value at the edges decreases along with reduction in variation between maximum and minimum stress values. Hence higher elastic modulus ratio (R) causes uniform shear stress distribution in the bond region.

Fig. 13 Out-of-plane normal stress (σ_z) distribution at mid-adhesive layer along bond radius for different elastic modulus ratios (R)
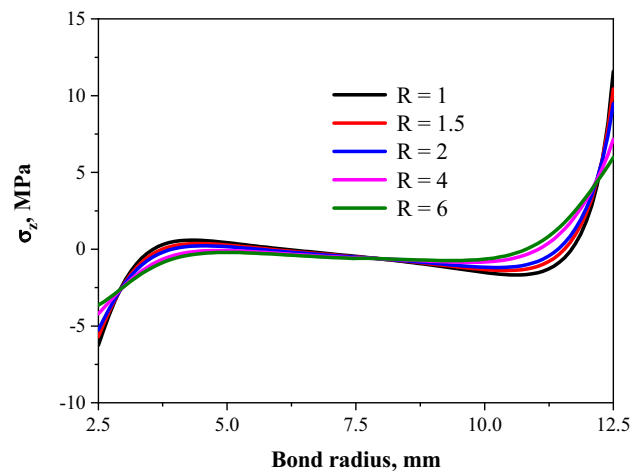
Fig. 14 Out-of-plane shear stress (τ_{yz}) distribution at mid-adhesive layer along bond radius for different elastic modulus ratios (R)
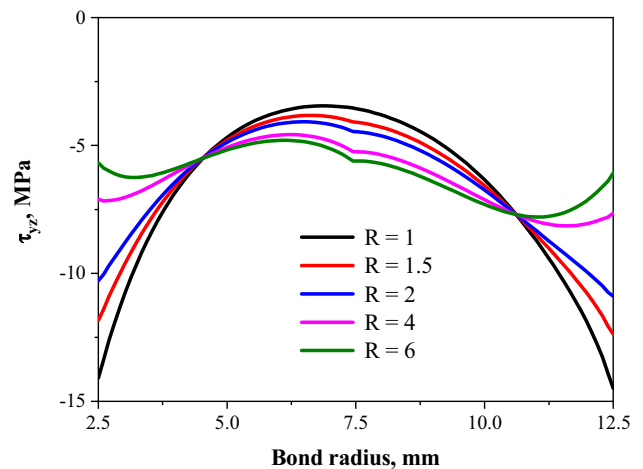

Fig. 15 Out-of-plane shear stress (τ_{xz}) distribution at mid-adhesive layer along bond radius for different elastic modulus ratios (R)
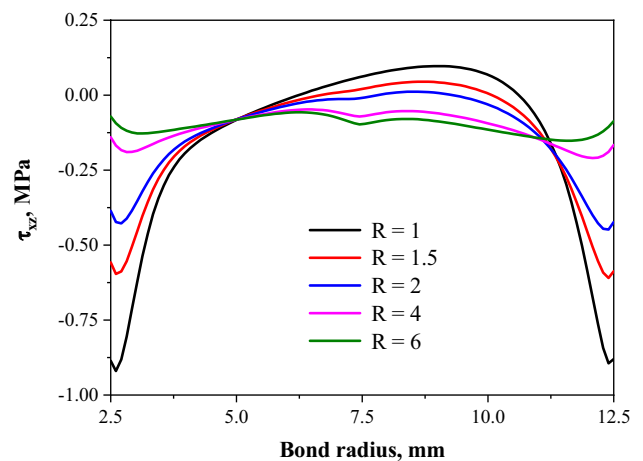

Table 5 shows values of the adhesive stresses at different adhesive interfaces for various modulus ratios at bond radius, $r = 2.5$ mm & 12.5 mm. It also shows reduction in adhesive peak stress for higher modulus ratios ($R = 6$) to that of mono modulus ($R = 1$) adhesive. The stress reduction (in percentage) is same across the thickness of adhesive due to gradation of adhesive elastic modulus. The two major stresses observed are normal stress (σ_z) and shear stress (τ_{yz}). The normal stress reduced by 41% and 48% at bond radius, $r = 2.5$ and $r = 12.5$ respectively. Similarly shear stress (τ_{yz}) component reduced by 59% due to gradation.

The reduction in stress observed is significant for elastic modulus ratio (R) of 6. For higher modulus ratio ($R > 6$) the more reduction in adhesive stress is possible. Hence, tailoring of adhesive elastic modulus along bond region will reduce stress concentration in the adhesive layer. This improves the joint strength and performance and failure onset in adhesive layer can be delayed drastically.

4 Conclusions

Present research work shows there is significant effect of functionally graded adhesive on the out-of-plane stresses induced at various interfaces of patch repaired system. Following specific conclusions made out of present research work are given below:

- For mono-modulus ($R = 1$) adhesive, out-of-plane normal and shear stresses in adhesive layer are not uniform. The adhesive normal stress (σ_z) varies from maximum negative value at bond radius ($r = 2.5$) to maximum positive value at bond radius ($r = 12.5$). It is more at the edges of hole and patch. This causes stress concentration in

Table 5 Out-of-plane stress values for different modulus ratios (R) at different bond radius (r) and at different interfaces of patch repaired system

Stress	r, mm	Interface	R = 1	R = 1.5	R = 2	R = 4	R = 6	Reduction (%)
σ_z	2.5	Adhesive-plate	−6.892	−6.284	−5.807	−4.638	−4.016	41.7
		Mid-adhesive layer	−6.249	−5.686	−5.253	−4.201	−3.639	41.8
		Adhesive-patch	−5.607	−5.088	−4.700	−3.765	−3.262	41.8
	12.5	Adhesive-plate	12.317	11.129	10.132	7.680	6.426	47.8
		Mid-adhesive layer	11.581	10.436	9.484	7.161	5.980	48.4
		Adhesive-patch	10.839	9.739	8.834	6.642	5.533	49.0
τ_{xz}	2.5	Adhesive-plate	−0.867	−0.546	−0.379	−0.138	−0.070	92.0
		Mid-adhesive layer	−0.886	−0.557	−0.386	−0.140	−0.071	92.0
		Adhesive-patch	−0.905	−0.568	−0.393	−0.143	−0.073	92.0
	12.5	Adhesive-plate	−0.858	−0.576	−0.417	−0.164	−0.086	90.0
		Mid-adhesive layer	−0.880	−0.587	−0.423	−0.166	−0.087	90.2
		Adhesive-patch	−0.902	−0.487	−0.430	−0.168	−0.087	90.3
τ_{yz}	2.5	Adhesive-plate	−14.028	−11.759	−10.222	−7.055	−5.648	59.7
		Mid-adhesive layer	−14.092	−11.832	−10.291	−7.099	−5.674	59.7
		Adhesive-patch	−14.151	−11.901	−10.357	−7.140	−5.699	59.7
	12.5	Adhesive-plate	−14.002	−12.021	−10.621	−7.525	−6.034	56.9
		Mid-adhesive layer	−14.485	−12.379	−10.896	−7.643	−6.088	58.0
		Adhesive-patch	−14.971	−12.738	−11.173	−7.762	−6.143	59.0

adhesive layer. The normal stress value is nearly constant or near to zero between bond radius (r = 5) and (r = 10). The adhesive shear stress (τ_{yz} & τ_{xz}) have maximum value at the edges.

- For different angular positions with loading axis adhesive stresses are varying. The adhesive normal stress (σ_z) has higher value in the loading axis, while it is lower for the direction perpendicular to the loading axis. Away from the edges of the hole and patch adhesive normal stress (σ_z) has negligible effect with the angular position along loading axis. The shear stress (τ_{yz}) component is varying from maximum negative value to maximum positive value from angular position of 0° to 180° with the loading axis and variation is a smooth curve. The shear stress (τ_{xz}) component varies from maximum negative value to maximum in positive value from angular position of 90° to 270° with the loading axis. Hence out-of-plane normal stress (σ_z) & shear stress (τ_{yz}) components have maximum value in the direction of the load while shear stress (τ_{xz}) component have maximum value in the direction perpendicular to the load.
- The pattern & nature of the adhesive stresses is similar along thickness of the adhesive but values of the stresses are different. At adhesive-plate interface, the value of adhesive normal stress (σ_z) is higher, while at adhesive-patch interface, the value of adhesive shear stress (τ_{yz} & τ_{yz}) is slightly higher as compared to other two positions along the thickness of the adhesive.
- Tailoring of adhesive across bond region reduces peak adhesive stresses. For mono- modulus adhesive, variation between maximum & minimum stress along bond region is higher. As the modulus ratio increases, the peak adhesive stress at the edges of hole and patch reduces. As the modulus ratio increases, the stress value at the edges decreases along with reduction in variation between maximum and minimum stress values. Hence, higher modulus ratio (R) causes uniform shear stress distribution in the bond region.
- The effect of reduction in peak adhesive stress at the stress concentration zone is promising, while away from stress concentration zone that is between bond radius (r = 5) to (r = 10) there is smaller change in the adhesive stress due to gradation of adhesive elastic modulus. Hence, at the edges where there is stress concentration zone, flexible adhesive can be used to reduce peak adhesive stress. Similarly at the interior, away from the edgesstiff adhesive can be usedtocarry more load.
- Due to functionally graded adhesive, reduction up to 59% in stress observed for elastic modulus ratio (R) of 6. For higher modus ratio (R > 6) the further more reduction in adhesive stress is possible. This reduces stress concentration in the adhesive layer and improves the strength and performance of patch repaired system. Furthermore, failure onset in adhesive layer can be delayed drastically. Hence, functionally graded adhesive is recommended for the designer of patch repaired system for its enhanced life and performance.

Declarations

Competing interests The author declares that there is no conflict of interest. There is no financial support to carry out the present work.

References

1. Tie Y, Ping Xu, Li C, Tian Z-Z. Effects of the initial adhesive disbonding on patch repaired composites. J Braz Soc Mech Sci Eng. 2018;40(4):225.
2. Kasavajhala L, Gu ARM, Zhao S. Finite element analysis of cracks in aging aircraft structures with bonded composite-patch repairs. Compos B Eng. 2011;42(3):505–10.
3. Marioli-Riga ZP, Gdoutos E. Composite patch repair methodology for damaged aircrafts structural components. SEM Annual Conference at Costa Mesa, California, USA. 2004.
4. Mohammadi S, Yousefi M, Khazaei M. A review on composite patch repairs and the most important parameters affecting its efficiency and durability. J Reinf Plast Compos. 2021;40(1–2):3–15.
5. Tsamasphyroset GJ, Kanderakis G, Karalekas D. Study of composite patch repair by analytical and numerical methods. Fatigue Fract Eng Mater Struct. 2001;24(10):631–6.
6. Rodríguez E, Mano R, Blanco L. Crack repair of steel vessels with bonded composite patches—damage control with FBGS. ECCM15 - 15th European Conference on Composite Materials, Venice, Italy. 2012.
7. Yang L, Yang Y, He S, Chen G, Ao C, Zhang W. Scarf patch repair of honeycomb sandwich composites and its simulation optimization. Plast, Rubber Compos. 2021;50(6):307–14.
8. Lee H, Seon S, Park S, Walallawita R, Lee K. Effect of the geometric shapes of repair patches on bonding strength. J Adhes. 2021;97(3):207–24.
9. Wang S, Xie Z, Li Z. On adhesively bonded stepped-scarf joint: an analytical model and its validation. Mech Adv Mater Struct. 2021;28(9):938–51.
10. Ghabezi P, Farahani M. A cohesive model with a multi-stage softening behavior to predict fracture in nano composite joints. Eng Fract Mech. 2019;229:106611.
11. Ghabezi P, Farahani M. Characterization of cohesive model and bridging laws in mode I and II fracture in nanocomposite laminates. J Mech Eng Sci. 2018;12(4):4329–55.
12. Vadean A, Abusrea M, Shazly M, Michel A, Kaabi A, Boukhili R. Improvement of scarf repair patch shape for composite aircraft structures. J Adhes. 2023;99(6):1044–70.
13. Shinde HP, Sonawane N, Karnik MG, Kumar P. Effect of patch length and elevated temperature on fatigue behaviour of repaired aluminium panels with a CFRP patch. J Adhes. 2023;99(10):1678–94.
14. Borges CSP, Akhavan-Safar A, Tsokanas P. From fundamental concepts to recent developments in the adhesive bonding technology: a general view. Discov Mech Eng. 2023;2(8):1–32.
15. Uslu M, Kaman MO. Progressive failure analysis of U-notched thin composite plates repaired with a double-sided composite patch. Proc Inst Mech Eng Part L J Mater Des Appl. 2023;237(5):1172–87.
16. Ghabezi P, Farahani M. Trapezoidal traction–separation laws in mode II fracture in nano-composite and nano-adhesive joints. J Reinf Plast Compos. 2018;37(11):780–94.
17. Moreira RDF, de Moura MFSF, Silva FGA. Quasi- static and fatigue analyses of aluminium structures repaired by CFRP patch bonding. Compos Struct. 2023;322:117372.
18. Truong VH, Kwak BS, Roy R, Kweon JH. Cohesive zone method for failure analysis of scarf patch-repaired composite laminates under bending load. Compos Struct. 2019;222:110895.
19. Carbas RJC, Viana GMSO, da Silva LFM, Critchlow GW. Functionally graded adhesive patch repairs of wood beams in civil applications. J Compos Constr. 2015;19(2):04014038.
20. Marques EAS, da Silva LFM. Joint strength optimization of adhesively bonded patches. J Adhes. 2008;84(11):915–34.
21. Breto R, Chiminelli A, Duvivier E, Lizaranzu M, Jiménez MA. Finite element analysis of functionally graded bond-lines for metal/composite joints. J Adhes. 2015;91(12):920–36.

22. Paroissien E, da Silva LFM, Lachaud F. Simplified stress analysis of functionally graded single-lap joints subjected to combined thermal and mechanical loads. Compos Struct. 2018;203:85–100.

23. Khan MA, Kumar S. Interfacial stresses in single-side composite patch-repairs with material tailored bond line. Mech Adv Mater Struct. 2017;25(4):304–18.

24. Srinivasan DV, Ravichandran V, Idapalapati S. Failure analysis of GFRP single lap joints tailored with a combination of tough epoxy and hyperelastic adhesives. Compos B Eng. 2020;200:108255.

25. Nimje SV, Panigrahi SK. Interfacial failure analysis of functionally graded adhesively bonded double supported tee joint of laminated FRP composite plates. Int J Adhes Adhes. 2015;58:70–9.

26. Dugbenoo E, Arif MF, Wardle BL, Kumar S. Enhanced bonding via additive manufacturing-enabled surface tailoring of 3D printed continuous-fiber composites. Adv Eng Mater. 2018;20(12):1800691.

27. Nakanouchi M, Sato C, Sekiguchi Y, Haraga K, Uno H. Development of application method for fabricating functionally graded adhesive joints by two-component acrylic adhesives with different elastic moduli. J Adhes. 2019;95(5–7):529–42.

28. Marques J, Barbosa A, Silva CI, Carbas R, da Silva LFM. An overview of manufacturing functionally graded adhesives- challenges and prospects. J Adhes. 2019;97:1–35.

29. da Silva CI, Cunha MRO, Barbosa AQ, Carbas RJC, Marques EAS, da Silva LFM. Functionally graded adhesive joints using magnetic microparticles with a polyurethane adhesive. J Adv Join Process. 2021;3:100048.

30. Rudawska A. The influence of curing conditions on the strength of adhesive joints. J Adhes. 2020;96(1–4):402–22.

31. Pourhassan S, Tavares PJ, Moreira PMGP. Material properties of 2024–T3 ALCLAD and 2124–T851 aluminum alloys using 2D and 3D Digital Image Correlation techniques. Procedia Struct Integr. 2017;5:1355–62.

32. Baker AA, Wang J. Adhesively bonded repair/reinforcement of metallic airframe components: materials, processes, design and proposed through-life management'. In: Jones R, Baker A, Matthews N, Champagne V, editors. Aircraft sustainment and repair. Boston: Butterworth-Heinemann; 2018. p. 191–252.

33. Nimje SV, Panigrahi SK. Numerical simulation for stress and failure of functionally graded adhesively bonded tee joint of laminated FRP composite plates. Int J Adhes Adhes. 2014;48:139–49.

34. Ravi Chandran KS, Barasom I. Determination of stress intensity factor solutions for cracks in finite-width functionally graded materials. Int J Fract. 2003;121:183–203.

35. Analas G, Lambros J, Santare MH. Dominance of a asymptotic crack-tip fields in elastic functionally graded materials. Int J Fract. 2002;115:193–204.

36. Nimje SV, Panigrahi SK. Proceedings of 56th Congress of Indian Society for theoretical and applied mechanics. Surat, India: SVNIT. 2011; 117–124.

37. Madani K, Touzain S, Feaugas X, Benguediab M, Ratwani M. Stress distribution in a 2024–T3 aluminum plate with a circular notch, repaired by a graphite/epoxy composite patch. Int J Adhes Adhes. 2009;29(3):225–33.